Stochastic model predictive control of an irrigation canal with integrated performance-driven path planning of a measurement robot

Ranjbar, Roza; García Martín, J.; Maestre, José María; Etienne, Lucien; Duviella, Eric; Camacho, Eduardo F.

DOI
10.2166/hydro.2025.300

Publication date
2025

Document Version
Final published version

Published in
Journal of Hydroinformatics

Citation (APA)
Ranjbar, R., García Martín, J., Maestre, J. M., Etienne, L., Duviella, E., & Camacho, E. F. (2025). Stochastic model predictive control of an irrigation canal with integrated performance-driven path planning of a measurement robot. *Journal of Hydroinformatics*, *27*(4), 740-754. https://doi.org/10.2166/hydro.2025.300

Journal of Hydroinformatics

Journal of Hydroinformatics Vol 00 No 0, 1 doi: 10.2166/hydro.2025.300

Stochastic model predictive control of an irrigation canal with integrated performance-driven path planning of a measurement robot

Roza Ranjbar [a], Javier G. Martin [b,*], Jose M. Maestre [c], Lucien Etienne [d], Eric Duviella [d] and Eduardo F. Camacho [c]

[a] Department of Economics, University of Waterloo, Waterloo, Canada
[b] Department of Maritime and Transport Technology, TU Delft, Delft, The Netherlands
[c] Department of Systems Engineering and Automation, University of Seville, Seville, Spain
[d] Department of CERI Digital Systems, IMT-Nord Europe, Lille, France
*Corresponding author. E-mail: j.garciamartin@tudelft.nl

RR, 0000-0003-2596-8897; JGM, 0000-0002-0362-5554; JMM, 0000-0002-4968-6811; LE, 0000-0003-0931-843X; ED, 0000-0002-1622-0994; EFC, 0000-0002-9636-5666

ABSTRACT

This work proposes a stochastic model predictive control for an irrigation canal with uncertainties where a moving robot takes measurements across the canal considering criteria such as the robot's velocity, energy consumption, and distances between the measuring spots. Tightened constraints are applied over the prediction horizon to the optimization so that the controller selects the optimal route for the robot from a control viewpoint. The simulations compare three different approaches, demonstrating that the proposed technique achieves superior results by reducing constraints violations and operational costs and ensuring more precise and reliable water level management across the canal compared to other methods.

Key words: automation, irrigation canal, moving robot, optimization, stochastic MPC

HIGHLIGHTS

- It proposes a control strategy that optimizes the operation of the water canal by considering predictive modeling and addressing uncertainties and constraints.
- The method employs a moving robot to take measurements at important spots of the irrigation canal.
- It involves planning the movement of the robot.
- The approach is useful in case of the low price of the deployment and maintenance of such a network.

GRAPHICAL ABSTRACT

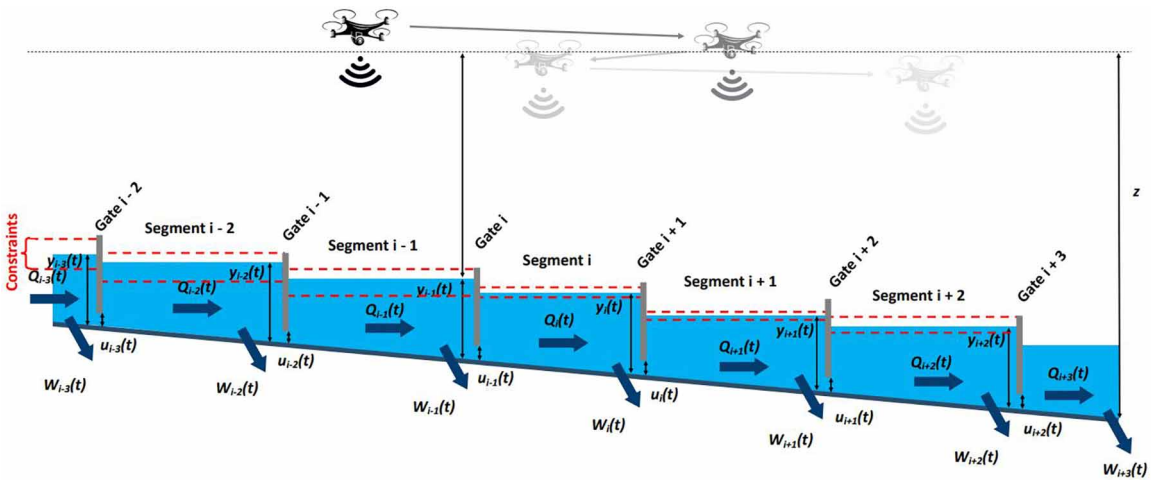

1. INTRODUCTION

Water systems must allocate the available water resources to provide farmers with water while keeping the level of each pool close to the set points (Segovia *et al.* 2019; Ranjbar *et al.* 2022; Shahverdi *et al.* 2022).

In this regard, there are challenges as the uncertainties arising from external disturbances, e.g., the inflows and human activities (Van Overloop *et al.* 2008), the errors of water level or flow measurements (Alam & Bhutta 2004), and modeling potential inaccuracies (Muleta & Nicklow 2005).

Many automation strategies have been proposed for water systems, e.g., model predictive controllers (MPCs), PID controllers, and linear quadratic regulators (LQRs) (Lozano *et al.* 2010; Kakouei *et al.* 2019; Hosseini Jolfan *et al.* 2020). In particular, MPC has demonstrated significant performance in the field of water systems management compared to other methods (Fele *et al.* 2014; Rodríguez *et al.* 2017; Segovia Castillo *et al.* 2018; Segovia *et al.* 2019; Pour *et al.* 2022). It is an optimization-based control strategy that uses a process model to predict the future behavior of a system for a certain prediction horizon while managing challenging issues such as constraints and delays (Figueiredo *et al.* 2013). In the case of irrigation canals, this approach requires a model of the canal dynamics and a forecast of future water demands. The model is employed to formulate an optimization problem, yielding the most efficient series of actions applicable to the system, guided by a performance index that aligns with operational objectives, such as maintaining the water level close to the designated set points (Ouarda & Labadie 2001; Geletu *et al.* 2013; Grosso *et al.* 2014; Velarde *et al.* 2019). Also, to deal with random disturbances in the system evolution, stochastic MPC (SMPC) has been introduced (Van Overloop 2006; Cannon *et al.* 2010; Nasir *et al.* 2017). One particular approach within the SMPC family is that of Chance-Constraint (Schwarm & Nikolaou 1999), which uses probabilistic information about additive disturbances to achieve a trade-off between constraint satisfaction and control performance (Cannon *et al.* 2012). Considering the stochastic features of the uncertainties, the method can set the frequency of constraint violations to be lower than a specified threshold (Dai *et al.* 2016).

To operate irrigation canals, sensors are needed to provide measurements, e.g., of water levels and flows (van de Wiel *et al.* 2020; Hamdi *et al.* 2021). Maintaining these sensors is costly and requires effort as they are prone to deterioration due to extreme weather conditions (Maestre 2021). In this regard, this work considers using a robot as a substitute for sensors. In particular, it is assumed that the robot can move freely around the system to capture measurements at different spots and transmit this information back to the controller. In areas where the robot is absent, the system model is used to provide the values following an unknown input observer (UIO) approach (Chen & Saif 2006; Conde *et al.* 2021). Additionally, the MPC algorithm also needs to consider the robot's velocity, battery, energy consumption, recharge, and the maximum distance between the spots to determine the robot routes.

Several studies have explored the use of robotic data collection methods. In the agricultural field, Tokekar *et al.* (2016) employed small and affordable unmanned aerial vehicles (UAVs) and unmanned ground vehicles (UGVs) together to collect soil data. Another study investigated the allocation of measurement tasks to multiple robots in a solar thermal plant (Martin *et al.* 2021a). Furthermore, in the same domain, Martin *et al.* (2021b) studied how the robot sensor network (RSN) can be managed to collect information for the control system while also updating the probability of coverage in specific areas of the solar field to direct the robots to locations where information collection was maximized. In Wang *et al.* (2016), a solution is proposed including a mobile robot and a path generation system to direct the robot's movements, taking into account the robot's expected deployment time, expected measurement value at each location, and the last time each location was visited. Most of the previous research regarding using mobile robots to monitor the water systems has focused on managing water quality (Von Borstel *et al.* 2013; Shademani *et al.* 2017; Anderson *et al.* 2022a, 2022b); however, the main contribution of this paper is employing a moving robot in a water canal that takes measurements of water levels at specific locations and the focus is exclusively on the water regulation problem. The fact that irrigation canals are exposed to external disturbances and retain random uncertainty motivated the development of a stochastic MPC to plan the movement of the robot. The objective can be achieved by reducing constraint violations through tighter constraints and improved control performance.

Preliminary research of the current work has been presented in Ranjbar *et al.* (2023). By addressing the identified gaps and limitations of this paper, the new study contributes to novel perspectives in this field. We apply the existing strategy to an extended model of the canal, rather than a portion of it. Additionally, the functional features of the robot have been taken into account, enhancing the practicality of our work. The current investigation incorporates parameters such as battery

level and maximum velocity, which impose restrictions on the robot's possible routes. Furthermore, the consideration of idle time necessitates an energy recharging period as an additional limiting factor. Finally, the current work updates the computation of uncertainty propagation along the prediction horizon.

The rest of the paper is organized as follows: Section 2 describes the system and the problem statement. In Section 3, the stochastic MPC framework and its interaction with the moving robot are explained. Simulation and results are presented in Section 4, followed by concluding remarks in Section 5.

2. PROBLEM STATEMENT

In this work, the Integrator-Delay (ID) model (Litrico & Fromion 2004) is employed to represent the dynamics of open-channel irrigation canals. This simplified model captures key hydraulic processes such as flow propagation, attenuation, and backwater effects, providing an accurate approximation of the Saint-Venant equations in both frequency and time domains. The ID model explicitly incorporates the influence of canal geometry, hydraulic structures, and physical parameters, enabling effective control design. The model accounts for variations in water levels $\Delta h(k)$ based on upstream and downstream flow rates $q_u(k-\tau_R)$ and $q_d(k)$, the backwater surface area (A_s), and the delay time (τ_R), critical for managing irrigation systems.

The simple discrete-time linear model for each canal pool is given by Arauz *et al.* (2020) as:

$$\Delta h(k) = \frac{T_s}{A_s}[q_u(k-\tau_R) - q_d(k)], \tag{1}$$

Note that this model establishes a canal pool featuring an initial section with regular depth, followed by the remaining section experiencing backwater conditions. Model parameters are computed by performing tests with the system starting in a steady-state condition, leading to the following general discrete-time linear model integrating the aspects of the hydrological cycle, such as rainfall and evaporation, as well as operational impacts from irrigation demand and agricultural withdrawals:

$$x(k+1) = A \cdot x(k) + B \cdot u(k) + D \cdot w(k), \tag{2}$$

$$y(k) = C(k) \cdot x(k), \tag{3}$$

where $x(k) \in \mathbb{R}^{n_x}$ stands for the state vector comprising water levels and flows within the canal relative to their respective set points; $u(k) \in \mathbb{R}^{n_u}$ denotes the input vector representing the changes in water flows, e.g., when there are operations in the hydraulic infrastructure such as gates; $w(k) \in \mathbb{R}^{n_w}$ stands for disturbances such as rainfalls, evaporation, agricultural activities, etc; and $y(k) \in \mathbb{R}^{n_y}$ is an output variable measured by a robot at time k from one of the designated measurement locations. Matrices derived from the ID model have the following dimensions: $A \in \mathbb{R}^{n_x \times n_x}$, $B \in \mathbb{R}^{n_u \times n_x}$, $C(k) \in \mathbb{R}^{1 \times n_x}$, and $D \in \mathbb{R}^{n_x \times n_w}$.

Note that supplementary components involving delayed flow measurements are present in the state to address the impact of the time it takes for water to traverse the canals within a discrete-time controller. For instance, a canal system featuring three pools and factoring in these additional elements might possess a state vector denoted as $x(k)$ in the following manner:

$$x(k) = \begin{bmatrix} \Delta e_1(k) \\ \Delta u_1(k-2) \\ \Delta u_1(k-1) \\ \Delta e_2(k) \\ \Delta u_2(k-1) \\ \Delta e_3(k) \\ e_1(k-1) \\ e_2(k-1) \\ e_3(k-1) \end{bmatrix} \tag{4}$$

where $\Delta e_i(k)$ for $i = 1, \ldots, 3$ refer to fluctuations in water-level discrepancy at time step k in pools 1, 2 and 3, respectively; $e_i(k)$ for $i = 1, \ldots, 3$ are water-level errors at time step k in pools 1, 2 and 3, respectively; and $\Delta u_i(k-1)$ and $\Delta u_i(k-2)$ for $i = 1, 2$ are control actions performed at the previous time step in pools 1 and 2, respectively.

The control objective is to minimize the following stage cost:

$$\ell(k) = x^{\mathrm{T}}(k+1) \cdot Q \cdot x(k+1) + u^{\mathrm{T}}(k) \cdot R \cdot u(k), \tag{5}$$

with weighting matrices $Q \in \mathbb{R}^{n_x \times n_x}$, $Q \succ 0$, and $R \in \mathbb{R}^{n_u \times n_u}$, $R \succ 0$, respectively. By minimizing $\ell(k)$ along a certain horizon (N_p), MPC can find the optimal sequence of inputs to apply to the system (2). The goal of this optimization is to minimize the fluctuations in water levels and flows with respect to their set point.

To this end, the optimization is performed considering that the states and inputs of the system are each subject to constraint sets as:

$$x \in \mathcal{X} = \prod_{i=1}^{N} \mathcal{X}_i, \quad u \in \mathcal{U} = \prod_{i=1}^{M} \mathcal{U}_i,$$

which contain the origin in their interior. These sets represent the physical boundaries of the respective values in each section of the canal, such as upper and lower limits for water levels and flows, for instance. In this regard, $\mathcal{X}_i = \{x_i \in \mathbb{R} : x_{i_{\min}} < x_i < x_{i_{\max}}\}$, and $\mathcal{U}_i = \{u_i \in \mathbb{R} : u_{i_{\min}} < u_i < u_{i_{\max}}\}$.

2.1. Stochastic disturbances and constraints

The amount of water in the canal system is affected by uncertain factors and modeling errors such as precipitation and hydrological run-off process parameters (Van Overloop *et al.* 2008), increasing the probability of constraint.

In this work, disturbances are assumed to follow normal distribution so that $w_i(k) \sim \mathcal{N}(\mu_i, {\sigma_i}^2)$, where μ_i and ${\sigma_i}^2$ are the corresponding mean and variance of disturbance $i \in \{1, 2, \ldots, n_w\}$. Thus, $x(k)$ will also become a vector of normal variables that can be computed as Camacho & Alba (2013):

$$x(k) = A^k \cdot x(0) + \sum_{i=1}^{\mathrm{k}} A^i \cdot B \cdot u(k-i) + \sum_{i=1}^{\mathrm{k}} D^i \cdot B \cdot w(k-i), \tag{6}$$

with

$$x_i(k) = \mathcal{N}(\mu_{xi}(k), {\sigma_{xi}}^2(k)), \quad i \in \{1, 2, \ldots, n_x\}. \tag{7}$$

In this context, the mean and variance are provided as follows:

$$\begin{cases} \mu_{xi}(k+1) & = \sum_{j=1}^{n_x} a_{ij} \cdot \mu_{xj}(k) + \sum_{r=1}^{n_w} d_{ir} \cdot \mu_{wr}(k) + \sum_{s=1}^{n_u} b_{is} \cdot u_s(k) \\ \sigma_{xi}(k+1)^2 & = \sum_{j=1}^{n_x} a_{ij}^2 \cdot \sigma_{xj}(k)^2 + \sum_{r=1}^{n_w} d_{ir}^2 \cdot \sigma_{wr}(k)^2 \end{cases} \tag{8}$$

Here, a_{ij}, b_{is}, and d_{ir} denote the corresponding component of matrices A, B, and D, respectively. As can be seen, μ_{xi} is influenced by present control actions, the initial state variable value and the noise mean μ, and σ_{xi} grows due to the uncertainty of the disturbance σ_{wi}; however, if the robot takes a measurement of the corresponding variable, the value of σ_{xi} is reset to zero. Likewise, it is important to emphasize that when computing the variance, it is assumed that the random variables involved are independent. However, if they are not independent, the proposed calculation becomes an approximation as it overlooks the effects of covariance. In general, we have operated under the assumption that comprehensive data related to rainfall duration, evaporation levels, and farming activities are at our disposal. This crucial assumption forms the foundation for computing both the mean and variance of disturbances.

To preserve performance while ensuring a certain level of constraint satisfaction we follow a stochastic approach. Also, such an approach is preferable to the overly cautious min-max control which often leads to sub-optimal results. Since x_i is a Gaussian random variable, the probability of $P(x_i(k) \in \mathcal{X}_i) \geq \gamma$ can be enforced, where γ is a predefined probability

threshold. In particular, this probabilistic constraint can be implemented by setting new tightened bounds on x_i, i.e.,

$$x_{i_{\min}} \leq \underline{x_i} < x_i(k) < \overline{x_i} \leq x_{i_{\max}}, \tag{9}$$

where $\underline{x_i}$ and $\overline{x_i}$ represent the lower and upper limits on the corresponding state, respectively, and $x_{i_{\min}}$ and $x_{i_{\max}}$ are the minimum and maximum boundaries in $\mathcal{X}_i$ and $\mathcal{U}_i$, in sequence. It should be noted that states corresponding to water flows are not the target of the robot's measurement, although they are part of state vector $x(k)$. In this regard, the model matrices simply implement a delay mechanism for the representation of water flows, resulting in the inclusion of delayed inputs within the state vector.

The so-called chance constraints formulation takes the form:

$$\begin{cases} P[x_i(k) < \overline{x_i}] \geq 1 - \gamma_{x,i} \\ P[\underline{x_i} < x_i(k)] \geq 1 - \gamma_{x,i} \end{cases} \quad \forall\, i \in \mathbb{N}^{n_x}, \quad \forall\, k \tag{10}$$

That is, chance constraints guarantee that the constraints will be met with a minimum probability of $1 - [\gamma]_{x,i}$. In other words, Equation (10) restricts to $[\gamma]_{x,i}$ which is the probability of violating the linear state constraint i at future time $k+1$ by knowing the state x_k at time k (Grosso *et al.* 2014). The SMPC controller solves the following optimization problem (Nasir *et al.* 2019):

$$\min_{x} \quad J(x(k)) \tag{11}$$

$$\text{s. t.} \quad P_k\{w(k) \in D_k \,|\, \underline{x_i} < x_i(k) < \overline{x_i},\, (2)\} \geq 1 - \gamma_{x,i}, \tag{12}$$

where the constraint must be satisfied with a probability of $1 - \gamma_{x,i}$ concerning the stochastic aspects of the uncertain demand forecast (D_k, P_k).

2.2. Planning the robot's movement

The system is considered as a graph $\mathcal{G} = (\mathcal{V}, \mathcal{E})$ with $\mathcal{V} = \{1, 2, \ldots, N\}$ a set of measurement spots (where N is the last spot) and $\mathcal{E}$ representing a set of edges such that $(v_i, v_j) \in \mathcal{E}$ when there exists a direct route between v_i and v_j. To employ a robot to take measurements of water level at different spots, a route r has to be calculated from location $v_i \in \mathcal{V}$. A route is a sequence of edges $\{(v_i, v_j), (v_j, v_k), \ldots\}$ connecting a set of vertices to each other (Van Overloop *et al.* 2015). If the robot visits location v_i at time step k, a measurement is sent to the controller, so that $\sigma_{xi}(k) = 0$; otherwise, $\sigma_{xi}(k)$ keeps growing, ultimately compelling the robot to return to the specified location at a later time through the tightening of the constraints.

Let us define $\mathcal{R}_{vi}(n)$ as the set of all routes within the graph $\mathcal{G}$, with a length of n and commencing from the spot v_i. The most straightforward approach to creating the routes between these spots involves an exhaustive exploration of all possible combinations. This entails estimating the combinations of variables a total of $2^n - 1 = nv_i + nv_j + \cdots + nv_k + \cdots + nv_n$ times, where $n_v k$ represents the number of estimations required for combinations of k spots. This approach is referred to as the Exhaustive Search (ES) method in literature (Igarashi *et al.* 2016). While precise techniques such as ES offer optimal solutions, they inevitably incur significant computational complexity, which can pose challenges for real-time systems. Assuming that the robot can go from one spot to another during one sampling time, $R_{vi}(N_p)$ becomes the combination of set $\mathcal{V}$ with repetitions. Any route $r \in \mathcal{R}_{vi}(N_p)$ requires accounting for the issues of the robot. As the value of N_p increases, managing the computational demands of the ES method becomes progressively more challenging. Thus, to mitigate the computational burden, a reduced prediction horizon can be introduced as Figure 1 such that $N_{red} < N_p$, and

$$r \in \mathcal{R}_{v_i}(N_p - N_{red} \,|\, N_{red}) \tag{13}$$

This way, the exhaustive search among the routes is limited to the first $N_p - N_{red}$ time instants, that is $\mathcal{R}_{vi}(N_p - N_{red} \,|\, N_{red})$, which are then extended for N_{red} time steps assuming that the robot follows a deterministic route, visiting each measuring spot sequentially until the horizon ends (Igarashi *et al.* 2018). While the use of a reduced horizon helps reduce computational complexity, further optimizations are needed to ensure the approach remains feasible for real-time systems, especially as the problem size scales up.

To compute the tightening parameters, the Gaussian variable x_i is converted into a normalized Gaussian $Z = \mathcal{N}(0, 1)$. Then, its Cumulative Distribution Function (CDF) is employed to set how each limit is updated. Finally, let us denote the set of tightened constraints that correspond to route r by $\mathcal{X}_r(k)$.

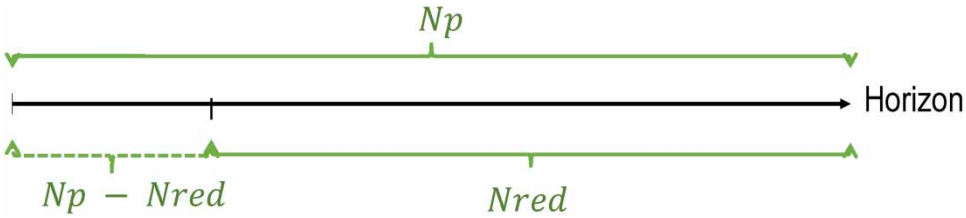

Figure 1 | Reduced prediction horizon.

3. PROPOSED ALGORITHM

In this section, the design of an SMPC and its interaction with the moving robot is presented. In this respect, it is important to take into account all the potential routes of the robot, followed by determining the optimal route. To do so, the optimization problem is formulated for each instance the robot sends a measurement from any spot $v \in \mathcal{V}$ as:

$$\min_{u(k:k+N_p-1),r} \quad J = \sum_{l=0}^{N_p} \ell(x(k+l+1), u(k+l)), \tag{14}$$

s. t.

$$x(l+1) = A \cdot x(l) + B(l) + w(l), \tag{15}$$

$$r \in \mathcal{R}_{v_i}(N_p - N_{red} \,|\, N_{red}) \tag{16}$$

$$u(l) \in \mathcal{U}, \tag{17}$$

$$x(l) \in \mathcal{X}_{r(l)} = f(x(k), r, \gamma) \quad \forall\, l \in [1, N_p] \tag{18}$$

Therefore, the optimization problem is solved at every time step considering the reduced prediction horizon, obtaining the inputs that are provided to the system $u(k:k+N_p-1)$ (17) and the best of the possible routes considered for the robot according to (16). However, only the first input is applied and the rest of the components are disregarded according to the receding horizon philosophy.

Remark 1. *Equation (18) emphasizes that the state constraints depend on the route by the fact that uncertainty grows with the number of time steps elapsed since the robot's last visit.*

The proposed approach followed at each time instant takes the form of Algorithm 1.

Algorithm 1 Online Calculations, Executed at Every Time Step k, $k \in N_p$ During the Sampling Time T_s

---

for each unit of distance, the robot's battery recharge for each sampling time, and the robot's fixed velocity.
Ensure: the current state *x(k)* in (6)
1: Compute the current robot's battery
2: Compute the set of possible routes $\mathcal{R}_{v_i}$
3: **for each** $r \in \mathcal{R}_{v_i}$ **do**
4: Define the set of tightened constraints $\mathcal{X}_{r(k+1:k+l+1)}$ according to γ and σ
5: Update the robot's battery
6: Compute J through MPC in (14)
7: **end for**
8: Select the optimum routes with the minimum J
9: Apply $u(k) = u^*(k)$
10: Recompute MPC for the next time steps.

Initially, the desired segment (reach) from which the robot should start traveling is selected. The starting spot for the robot may be arbitrarily chosen, with the option to commence from the beginning, middle, or end of the canal to undertake the measurements. This decision can be made based on various factors, such as the nature of the canal, accessibility, and the specific objectives of the measurement.

Following this, the system incorporates noise in the form of a vector containing the mean of each reach, denoted by μ_i, and the variance of disturbance represented by σ_i. Thus, by having the disturbances following the normal distribution, the current state $x(k)$ is computed by employing Equation (6).

After specifying the robot's velocity, the maximum distance it can traverse is calculated as $D = V.T_s$, where D represents the distance limit that the robot can cover, V denotes the velocity of the robot, and T_s corresponds to the sampling time. Next, the battery of the robot can be calculated for each route. To do so, the new battery level is determined by adding the current amount of battery to the amount of battery recharged and then subtracting the energy consumed during the distance traveled, which is multiplied by the energy consumption rate. As mentioned in Section 2.2, the robot's features play a crucial role in determining the total number of feasible routes for the robot. Consequently, the set of possible routes $\mathcal{R}_{v_i}$ is computed by taking into account the robot's restrictions and conducting an exhaustive search with the reduced prediction horizon N_{red}.

Once all the possible routes have been identified, for each route, the constraints on states get tightened based on the selected γ and the variable σ_i and there becomes a set of tightened constraints $\mathcal{X}_r(k)$. Additionally, at each sampling time, the robot's battery gets updated and the cost J is computed through the MPC formulation.

When the costs are determined for all available routes, the routes containing the minimum cost are deemed as the optimal choice. Subsequently, the updated inputs are incorporated into the MPC framework, triggering the recomputation of the process for subsequent time steps until the end of the prediction horizon.

4. RESULTS AND DISCUSSION

The proposed strategy is validated using a reference model, the case introduced in Clemmens *et al.* (1998), by the ASCE Task Committee on Canal Automation Algorithms as a standard case on canals with practical and realistic properties. This canal consists of eight different reaches and a schematic view of it is displayed in Figure 2. Since the distance between reaches 1 and

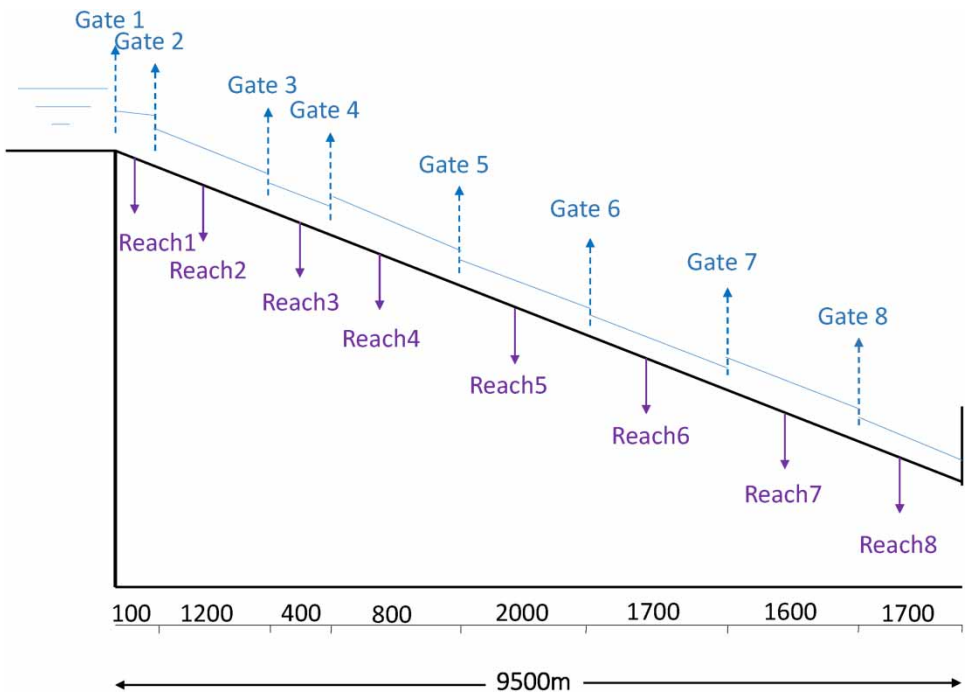

Figure 2 | Longitudinal profile of the ASCE Test Canal 1.

2 is too small, they are combined as a single node in our model. Furthermore, the canal has a total length of 9,500 m, and the size of each pool is depicted in the figure. The water levels are set above the normal depth.

For this research, a DJI-based drone, a type of unmanned aerial vehicle (UAV) known for its advanced capabilities and versatility, has been selected as the robot for the study. Given the total length of the canal, and the number of trips the robot is expected to make, its velocity is set to 15 m/s, as higher velocities result in greater energy consumption. The energy consumption for each unit of distance is considered to be the 0.003 state of charge (SoC), where SoC is a crucial indicator of battery condition determined by calculating the ratio between the remaining capacity and the total capacity of the battery (Sun *et al.* 2021). To this end, the initial battery of the robot is 40 SoC and the battery recharge is set to 2.5 SoC for each sampling time (Aguilar-López *et al.* 2022). Based on the fact that energy consumption is the product of distance traveled and energy consumed per unit distance, the total energy consumption for the drone can be calculated by multiplying the 9.5 km distance by the energy consumption rate of 0.003 SoC per meter. The flight time is determined by dividing the total distance by the drone's velocity, resulting in an approximately 20-min duration for a round trip of 19 km. The energy recharge rate also gives the drone a good amount of energy recovery during the trip. Considering these factors – the energy consumption for the round trip, the drone's flight time, and its recharge capabilities – the initial battery life of 40 SoC appears sufficient to successfully traverse the length of the canal. This setup ensures that the drone can complete multiple round trips while maintaining a reasonable margin of battery life for continued operation.

The robot is considered to start from the beginning of the canal in the first reach. The set point is $x = 0$ with an initial upper and lower bound equal to $\overline{x} = +1m$ and $\underline{x} = -1m$, for all eight reaches. The prediction horizon and the reduced prediction horizon are set to $N_p = 10$ and $N_{red} = 7$, respectively. The sampling time is selected as $T_s = 30$ min. For the stochastic disturbances, the variance is set to be a column vector of size n_w, where each element has a value of 0.3, and the mean is assigned a matrix with elements in the range of $(-0.6, +0.4)$ as in Figure 3.

The MPC optimization problem is solved for every route of the robot applying quadratic programming (QP). Matrix Q has ones in the states corresponding to water levels and zeros elsewhere, while matrix R is likewise diagonal, assigning a value of 0.2 to each control action (each reach of the canal that the measurements are taken from). The constraints are tightened by assuming a maximum probability violation of 0.01 (γ is selected to be 0.99). In order to assess the suggested methodology, two alternative algorithms are implemented in the system. One includes an MPC controller with a robot that moves sequentially

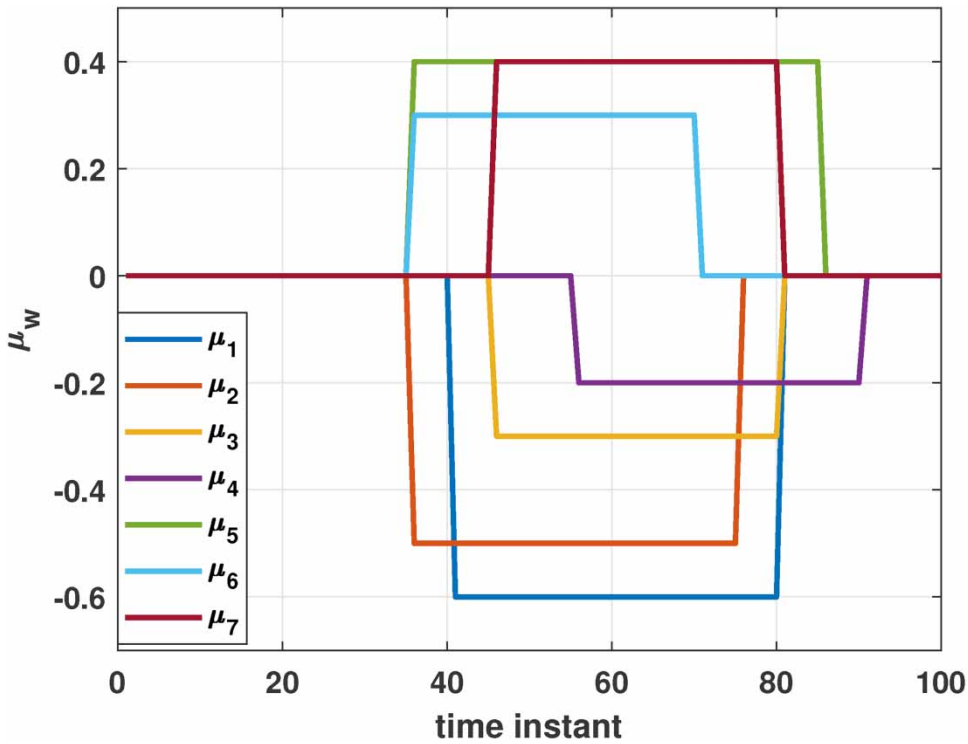

Figure 3 | The mean assigned to each disturbance of the canal.

following a predefined route that includes measuring all spots from the initial to the final point and then returning from the final point to the initial one (referred to as PR-MPC). The other method involves employing an MPC controller with classic constraints incorporating full system information (referred to as C-MPC). Our proposal is called the Optimal Route with Stochastic Constraints Model Predictive Control (SC-OR- MPC).

The water levels presented in the following figures correspond to the levels at seven reaches across the canal. The blue lines account for the states, the green lines are the belief states of the system, and the constraints (hard and soft tightened) are shown in dashed blue/green lines, respectively. As shown, advanced control schemes like MPC can suffer when the estimate of the real state of the system differs. In the context of this case study, with the robot providing updates of the state vector, there is a significant loss of performance and stability as demonstrated by the results of the PR-MPC method with hard constraints (in

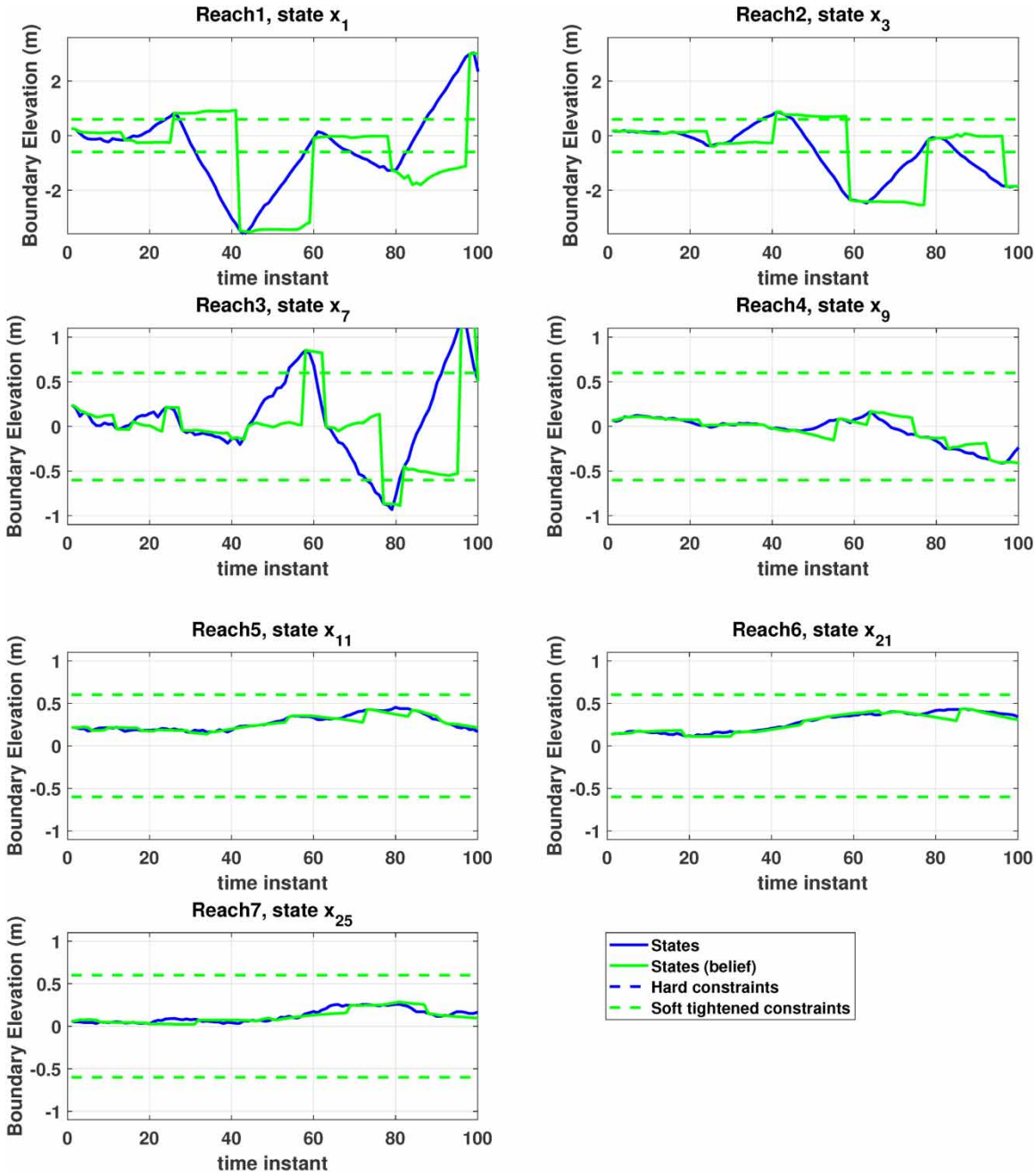

Figure 4 | Water levels without stochastic constraints: PR-MPC.

Figure 4). Likewise, when the constraints are not tightened , the uncertainty in the system evolution is not adequately accounted for by the controller's internal model. In Reach 1, applying only the MPC with a predefined route (PR-MPC) led to a violation of the constraints for 30 out of a 100 time instant period. However, when constraints were designed to tighten dynamically based on the time elapsed since the last measurement (in SC-PR-MPC), the violation duration was reduced to just 5 seconds (Figure 5), representing an %83.3 reduction. Furthermore, when smart movement was incorporated into the robot's strategy (Figure 6), constraint violations were nearly eliminated, with only negligible violations observed. A similar trend was observed in Reach 2 and Reach 3, where the introduction of stochastic constraints (SCs) and smart movement significantly improved the system's performance. Although the specific durations of violations varied, the overall outcomes showed a substantial reduction in constraint violations.

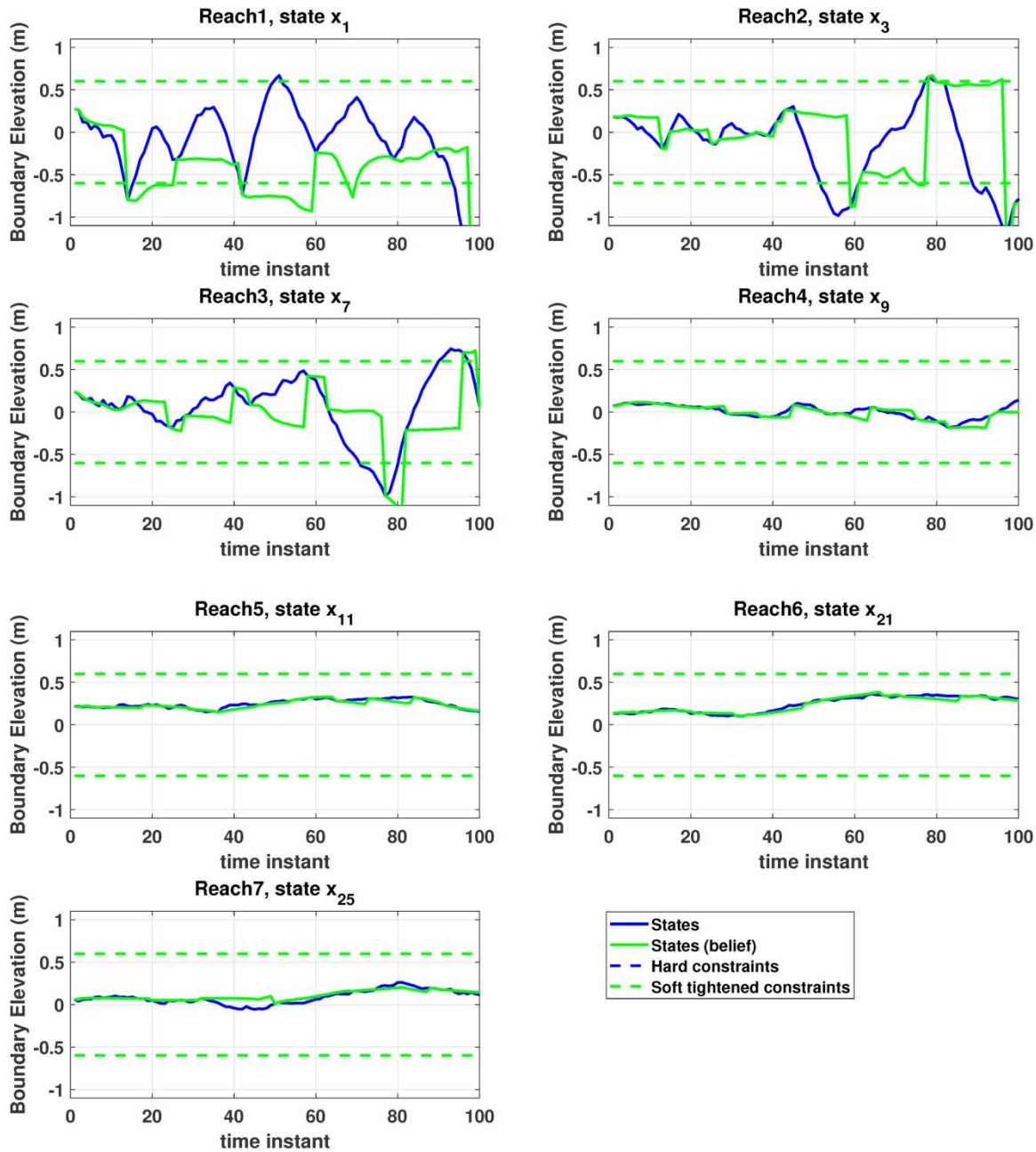

Figure 5 | Water levels with stochastic constraints in PR-MPC (SC-PR-MPC).

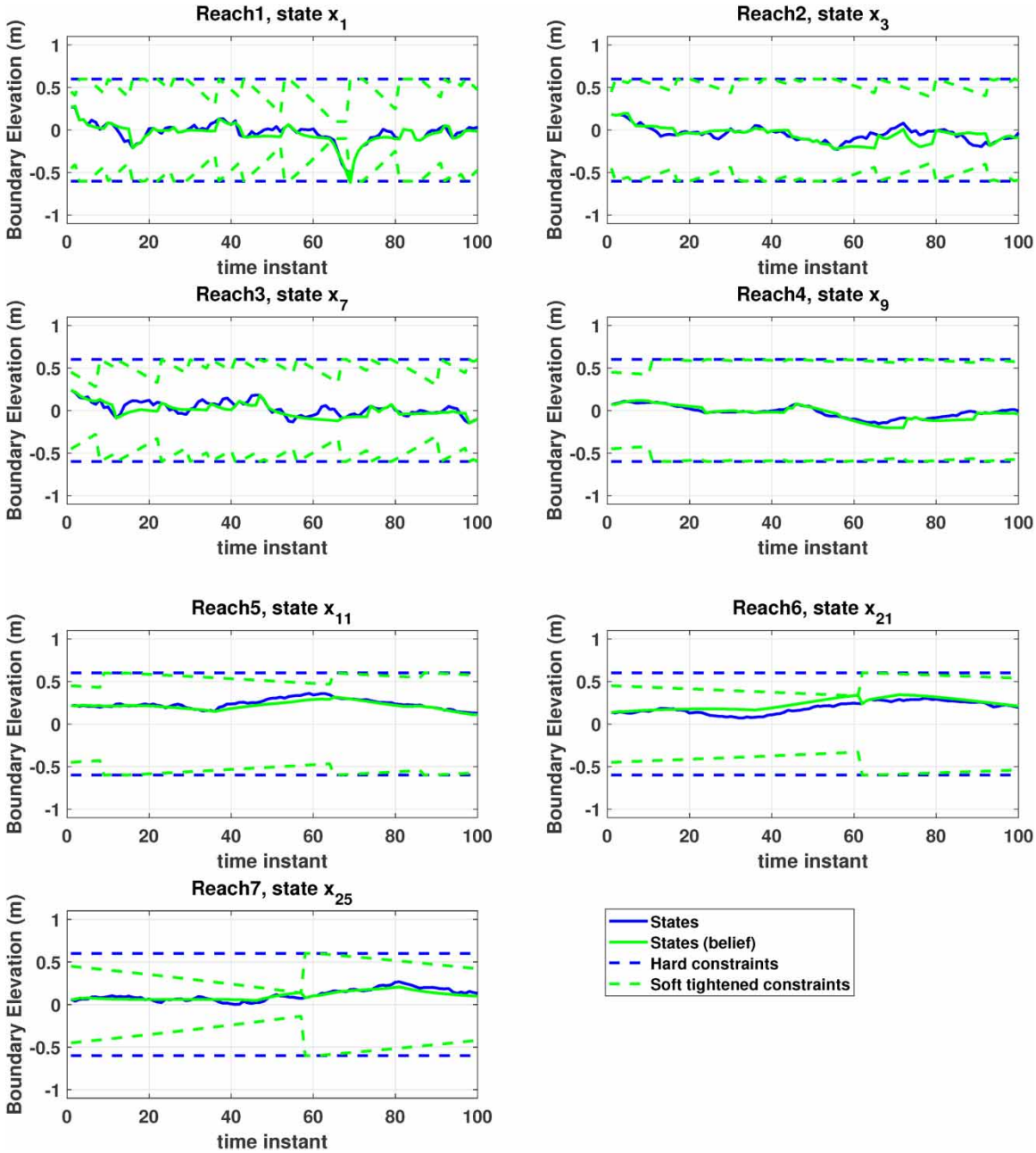

Figure 6 | Water levels with stochastic constraints in proposed method (SC-OR-MPC).

Thus the proposed method for tightening the constraints enhances the controller's ability to focus on the most uncertain states of the system. By tightening these constraints, the controller becomes more sensitive to potential deviations from the desired performance, which allows it to better prioritize areas of the system where uncertainty is the highest. As a result, the overall performance improves, as illustrated in Figure 5, where the PR-MPC method with tightened soft constraints (referred to as SC-PR-MPC) is shown. The tightening method reduces the discrepancy between the controller's predicted and actual states, leading to fewer violations of the system's constraints. However, despite this improvement, there is still significant room for further optimization. A key opportunity for enhancing performance lies in allowing the controller to autonomously select the measurement locations for the robot. By enabling the controller to decide where to gather data, it can maximize the utility of the robot's measurement capacity and available battery life. This approach would ensure that

the robot visits the most critical locations – such as gates or reaches that significantly impact the system's overall performance – thereby optimizing the use of resources and improving the controller's efficiency.

This concept is clearly demonstrated in Figure 6, which shows the results of the closed-loop system using the proposed SC-OR-MPC method. The figure highlights a notable improvement: While the two other methods assessed in the study result in multiple violations of constraints, the SC-OR-MPC approach reduces these violations to a single minor breach of a soft constraint (not a hard constraint) around time instant 70 at Reach 1 (x_1). Furthermore, there is a much closer alignment between the belief states and the actual states, indicating that the controller is better able to estimate the system's real-time conditions. The closer correspondence underscores the effectiveness of the tightened soft constraints and the optimized measurement strategy in improving overall system performance.

Table 1 presents the accumulated cost of the three assessed methods over the 100 time instants of the simulation. It also includes the results of a conventional MPC (C-MPC) controller with full state information, providing a reference of the loss of performance due to the absence of a fixed sensor network. Table 1 demonstrates that the proposed SC-OR-MPC method effectively compensates for the lack of a fixed sensing infrastructure. Despite not relying on a permanent sensor network, the proposed approach maintains performance close to that of the C-MPC controller.

Finally, Figure 7 displays the segments visited by SC-OR-MPC and PR-MPC methods and shows the evolution of the robot's battery over time. Unlike the sequential, predetermined visits of the PR-MPC method, the SC-OR-MPC allows for more flexible scheduling of the robot's visits to the segments. This flexibility is based on the robot's velocity and remaining battery capacity. As expected, the robot prioritizes the initial segments of the canal, as these are more critical for effective control

Table 1 | Accumulated cost in the assessed approaches vs. conventional MPC with full state information

Cost / Approach	Accumulated cost	Relative cost to C-MPC (%)
C-MPC	26.68	–
SC-OR-MPC	27.64	3.6
SC-PR-MPC	100.02	274.9
PR-MPC	441.84	1556.1

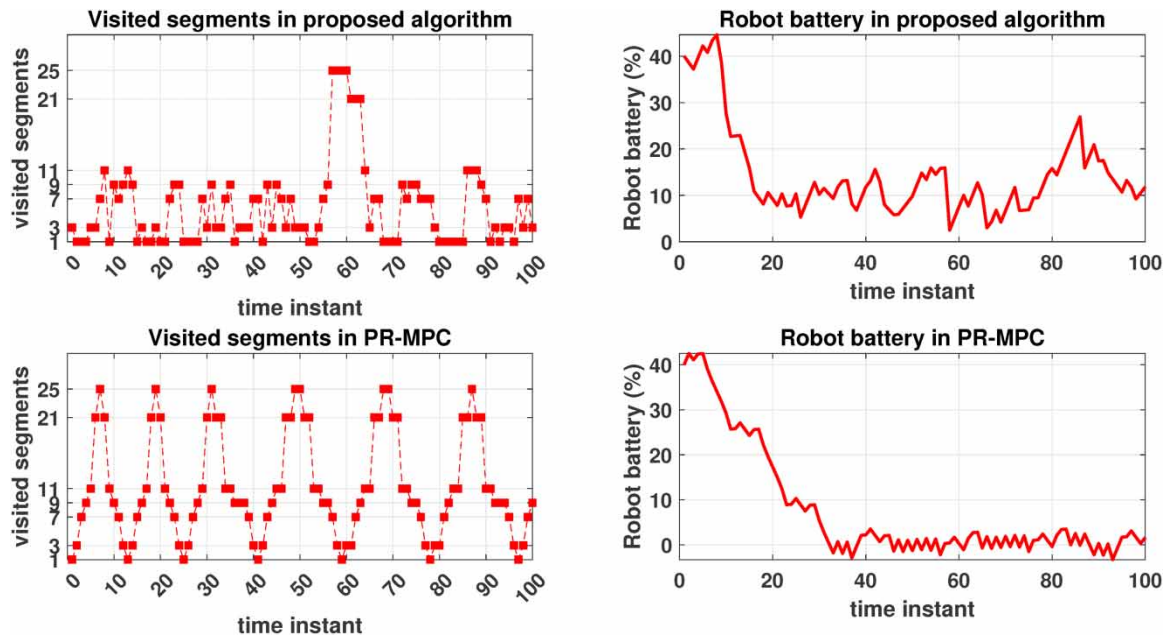

Figure 7 | Visited segments and robot battery in SC-OR-MPC and PR-MPC.

due to the canal's sequential structure. The system's performance is more sensitive to the initial reaches, meaning that early adjustments are crucial for maintaining optimal conditions throughout the canal. This explains why the robot makes repeated visits to the early segments, ensuring that the control objectives are met in a timely and efficient manner. The ability of the proposed algorithm to dynamically allocate visits based on real-time conditions, such as velocity and battery status, enhances the overall effectiveness of the system, allowing for more targeted interventions where they are most needed.

5. CONCLUSION

In this work, a moving robot in combination with a stochastic MPC is applied to the ASCE test canal. The canal is considered to have uncertainties and the moving robot is planned to move along the reaches and take measurements right at reaches. To do so, the movement of the robot is limited to its battery, velocity, energy consumption, and the distances it can travel. The controller selects the optimal routes for the robot by tightening the constraints at every sampling time of the prediction horizon. The performance has been evaluated by comparing the proposed algorithm with a classic MPC with no uncertainty and another proposal that assigns a robot moving through predefined routes. The outcome of this work highlights the favorable control performance of the proposed approach, in terms of economic efficiency compared to other approaches. Moreover, the method effectively compensates for the lack of a fixed sensor network infrastructure by providing essential information to the controller to minimize constraints violations. Considering the price of the deployment and maintenance of such a network, the proposed alternative based on a controlled robot that retrieves water level measurements should be fully taken into account in water management projects.

Future work will explore how this robot can be integrated with operators in the loop, enabling the benefits of model predictive control to be realized without the need for installing fixed actuators and sensors in the irrigation canal. Additionally, we aim to investigate reinforcement learning-based approaches and other methods like neural network-based controllers to enhance the adaptability and robustness of the control strategy, providing a richer comparative framework and deeper insights into the proposed method's performance. Moreover, to address the computational complexity of the Exhaustive Search (ES) method, we plan to explore optimizations such as reducing the prediction horizon further and using heuristic methods to make the search more efficient for real-time applications.

FUNDING

This project received funding from the European Research Council (ERC) under the European Union's Horizon 2020 research and innovation program (OCONTSOLAR, grant agreement no. 789051) and the C3PO projects corresponding to grant PID2020-119476RB-I00, and grant PID2023-152876OB-I00 funded by MCIN/AEI/10.13039/501100011033 and ERDF/EU. Additionally, it is supported by the Regional Council of Hauts-de-France. The authors gratefully thank these institutions for their support.

AUTHOR CONTRIBUTIONS

All authors contributed to the study's conception and design. R.R. contributed to methodology, coding, data processing, validation, writing – original draft, writing – review and editing. J.G.M. contributed to coding, visualization, collected resources, writing – review and editing. J.M.M. contributed to supervision, coding, methodology, review and editing. L.E. contributed to resources. E.D. contributed to review and editing. E.F.C. contributed to review and editing.

DATA AVAILABILITY STATEMENT

All relevant data are included in the paper or its Supplementary Information.

CONFLICT OF INTEREST

The authors declare there is no conflict.

REFERENCES

Aguilar-López, J. M., García, R. A., Bordons, C. & Camacho, E. F. (2022) 'Development of the energy consumption model of a quadrotor using voltage data from experimental flights', In: *2022 IEEE 17th International Conference on Control & Automation* Naples, 27–30 June 2022. New York, NY: IEEE, pp. 432–437.

Alam, M. & Bhutta, M. (2004) Comparative evaluation of canal seepage investigation techniques, *Agricultural Water Management*, **66** (1), 65–76.

Anderson, A., Martin, J., Bouraqadi, N., Etienne, L., Fabresse, L., Langueh, K., Lozenguez, G., Rajaoarisoa, L., Maestre, J. & Duviella, E. (2022a) Map meshing impact on the efficiency of nonlinear set-based model predictive control for water quality assessment, *IFAC-PapersOnLine*, **55** (33), 105–110.

Anderson, A., Martin, J., Mougin, J., Bouraqadi, N., Duviella, E., Etienne, L., Fabresse, L., Langueh, K., Lozenguez, G., Alary, C., Billon, G., Superville, P. & Maestre, J. (2022b) Water quality map extraction from field measurements targeting robotic simulations, *IFAC-PapersOnLine*, **55** (5), 1–6.

Arauz, T., Maestre, J. M., Tian, X. & Guan, G. (2020) Design of pi controllers for irrigation canals based on linear matrix inequalities, *Water*, **12** (3), 855.

Camacho, E. F. & Alba, C. B. (2013) *Model Predictive Control*. Cham: Springer Science & Business Media.

Cannon, M., Kouvaritakis, B., Raković, S. V. & Cheng, Q. (2010) Stochastic tubes in model predictive control with probabilistic constraints, *IEEE Transactions on Automatic Control*, **56** (1), 194–200.

Cannon, M., Cheng, Q., Kouvaritakis, B. & Raković, S. V. (2012) Stochastic tube MPC with state estimation, *Automatica*, **48** (3), 536–541.

Chen, W. & Saif, M. (2006) 'Unknown input observer design for a class of nonlinear systems: an LMI approach', *2006 American Control Conference*, Minneapolis, MN, 14–16 June 2006. New York, NY: IEEE.

Clemmens, A., Kacerek, T., Grawitz, B. & Schuurmans, W. (1998) Test cases for canal control algorithms, *Journal of irrigation and drainage engineering*, **124** (1), 23–30.

Conde, G., Quijano, N. & Ocampo-Martinez, C. (2021) 'An unknown input moving horizon estimator for open channel irrigation systems', *2021 European Control Conference (ECC)*, Rotterdam, 29 June – 2 July 2021. New York, NY: IEEE, pp. 1249–1254.

Dai, L., Xia, Y., Gao, Y. & Cannon, M. (2016) Distributed stochastic mpc of linear systems with additive uncertainty and coupled probabilistic constraints, *IEEE Transactions on Automatic Control*, **62** (7), 3474–3481.

Fele, F., Maestre, J. M., Hashemy, S. M. & Camacho, E. F. (2014) Coalitional model predictive control of an irrigation canal, *Journal of Process Control*, **24** (4), 314–325.

Figueiredo, J., Botto, M. A. & Rijo, M. (2013) Scada system with predictive controller applied to irrigation canals, *Control Engineering Practice*, **21** (6), 870–886.

Geletu, A., Klöppel, M., Zhang, H. & Li, P. (2013) Advances and applications of chance-constrained approaches to systems optimisation under uncertainty, *International Journal of Systems Science*, **44** (7), 1209–1232.

Grosso, J., Ocampo-Martínez, C., Puig, V. & Joseph, B. (2014) Chance-constrained model predictive control for drinking water networks, *Journal of process control*, **24** (5), 504–516.

Hamdi, M., Rehman, A., Alghamdi, A., Nizamani, M. A., Missen, M. M. S. & Memon, M. A. (2021) Internet of things (iot) based water irrigation system, *International Journal of Online & Biomedical Engineering*, **17** (5), 69–80.

Hosseini Jolfan, M., Hashemy Shahdany, S. M., Javadi, S., Mallakpour, I. & Neshat, A. (2020) Effects of canal automation on reducing groundwater extraction within irrigation districts: Case study of qazvin irrigation district, *Irrigation and Drainage*, **69** (1), 11–24.

Igarashi, Y., Nagata, K., Kuwatani, T., Omori, T., Nakanishi-Ohno, Y. & Okada, M. (2016) Three levels of data-driven science, *Journal of Physics: Conference Series*, **699**, 012001. IOP Publishing.

Igarashi, Y., Takenaka, H., Nakanishi-Ohno, Y., Uemura, M., Ikeda, S. & Okada, M. (2018) Exhaustive search for sparse variable selection in linear regression, *Journal of the Physical Society of Japan*, **87** (4), 044802.

Kakouei, S., Emadi, A. & Gholami Sefidkouhi, M. A. (2019) Application of pid controller for water level tuning (case study: Main canal of alborz irrigation network), *Irrigation and Drainage Structures Engineering Research*, **20** (75), 17–32.

Litrico, X. & Fromion, V. (2004) Simplified modeling of irrigation canals for controller design, *Journal of irrigation and drainage engineering*, **130** (5), 373–383.

Lozano, D., Arranja, C., Rijo, M. & Mateos, L. (2010) Simulation of automatic control of an irrigation canal, *Agricultural water management*, **97** (1), 91–100.

Maestre, J. M. (2021) Human in the loop model predictive control methods for water systems, *Systems, Control and Information*, **65** (9), 352–357.

Martin, J. G., Frejo, J. R. D., García, R. A. & Camacho, E. F. (2021a) Multi-robot task allocation problem with multiple nonlinear criteria using branch and bound and genetic algorithms, *Intelligent Service Robotics*, **14** (5), 707–727.

Martin, J., Maestre, J. & Camacho, E. (2021b) Spatial irradiance estimation in a thermosolar power plant by a mobile robot sensor network, *Solar Energy*, **220**, 735–744.

Muleta, M. K. & Nicklow, J. W. (2005) Sensitivity and uncertainty analysis coupled with automatic calibration for a distributed watershed model, *Journal of hydrology*, **306** (1–4), 127–145.

Nasir, H. A., Cantoni, M. & Weyer, E. (2017) 'An efficient implementation of stochastic MPC for open channel water-level planning', *2017 IEEE 56th Annual Conference on Decision and Control (CDC)*, Melbourne, 12–15 December 2017. New York, NY: IEEE, pp. 511–516.

Nasir, H. A., Cantoni, M., Li, Y. & Weyer, E. (2019) Stochastic model predictive control based reference planning for automated open-water channels, *IEEE Transactions on Control Systems Technology*, **29** (2), 607–619.

Ouarda, T. B. & Labadie, J. W. (2001) Chance-constrained optimal control for multireservoir system optimization and risk analysis, *Stochastic environmental research and risk assessment*, **15**, 185–204.

Pour, F. K., Segovia, P., Etienne, L. & Duviella, E. (2022) An mhe-based mpc strategy for simultaneous energy generation maximization and water level management in inland waterways, *IFAC-PapersOnLine*, **55** (33), 20–26.

Ranjbar, R., Etienne, L., Duviella, E. & Maestre, J. M. (2022) Sensitivity analysis of the digital twin of the canal of calais to the outlet gate modelling. In: *Advances in Hydroinformatics: Models for Complex and Global Water Issues–Practices and Expectations*. Cham: Springer. pp. 175–194.

Ranjbar, R., Martin, J. G., Maestre, J. M., Etienne, L., Duviella, E. & Camacho, E. F. (2023) 'Mobile robot model predictive control approach: case study of an irrigation canal', *2023 8th International Conference on Control and Robotics Engineering (ICCRE)*, Niigata, 21–23 April 2023. New York, NY: IEEE.

Rodríguez, F. L., Horváth, K., Martín, J. G. & Maestre, J. (2017) Mobile model predictive control for the évora irrigation test canal, *IFAC-PapersOnLine*, **50** (1), 6570–6575.

Schwarm, A. T. & Nikolaou, M. (1999) Chance-constrained model predictive control, *AIChE Journal*, **45** (8), 1743–1752.

Segovia, P., Rajaoarisoa, L., Nejjari, F., Duviella, E. & Puig, V. (2019) Model predictive control and moving horizon estimation for water level regulation in inland waterways, *Journal of Process Control*, **76**, 1–14.

Segovia Castillo, P., Rajaoarisoa, L., Nejjari, F., Duviella, E. & Puig, V. (2018) Distributed input-delay model predictive control of inland waterways.

Shademani, S., Zarafshan, P., Khashechi, M., Kianmehr, M. & Hashemy, S. (2017) 'Design and analysis of a dredger robot for covered irrigation canals', *2017 5th RSI International Conference on Robotics and Mechatronics (ICRoM)*, Tehran, 25–27 October 2017. New York, NY: IEEE, pp. 162–167.

Shahverdi, K., Alamiyan-Harandi, F. & Maestre, J. (2022) Double q-pi architecture for smart model-free control of canals, *Computers and Electronics in Agriculture*, **197**, 106940.

Sun, D., Yu, X., Wang, C., Zhang, C., Huang, R., Zhou, Q., Amietszajew, T. & Bhagat, R. (2021) State of charge estimation for lithium-ion battery based on an intelligent adaptive extended kalman filter with improved noise estimator, *Energy*, **214**, 119025.

Tokekar, P., Vander Hook, J., Mulla, D. & Isler, V. (2016) Sensor planning for a symbiotic uav and ugv system for precision agriculture, *IEEE Transactions on Robotics*, **32** (6), 1498–1511.

van de Wiel, L., van Es, D. M. & Feelders, A. (2020) Real-time outlier detection in time series data of water sensors. In: *Advanced Analytics and Learning on Temporal Data: 5th ECML PKDD Workshop, AALTD 2020, Ghent, Belgium, September 18, 2020, Revised Selected Papers 6*. Cham: Springer. pp. 155–170.

Van Overloop, P.-J. (2006) *Model Predictive Control on Open Water Systems*. Clifton, VA: IOS Press.

Van Overloop, P.-J., Weijs, S. & Dijkstra, S. (2008) Multiple model predictive control on a drainage canal system, *Control Engineering Practice*, **16** (5), 531–540.

Van Overloop, P., Maestre, J., Sadowska, A. D., Camacho, E. F. & De Schutter, B. (2015) Human-in-the-loop model predictive control of an irrigation canal [applications of control], *IEEE Control Systems Magazine*, **35** (4), 19–29.

Velarde, P., Tian, X., Sadowska, A. & Maestre, J. (2019) Scenario-based hierarchical and distributed mpc for water resources management with dynamical uncertainty, *Water Resources Management*, **33**, 677–696.

Von Borstel, F. D., Suárez, J. & Gutiérrez, J. (2013) Feeding and water monitoring robot in aquaculture greenhouse, *Industrial Robot: An International Journal*, **40** (1), 10–19.

Wang, R., Veloso, M. & Seshan, S. (2016) 'Active sensing data collection with autonomous mobile robots', In: *2016 IEEE International Conference on Robotics and Automation (ICRA)*, Stockholm, 16–21 May 2016. New York, NY: IEEE, pp. 2583–2588.

First received 21 October 2024; accepted in revised form 20 March 2025. Available online 2 April 2025